Food Chemistry 294 (2019) 203–208

Contents lists available at ScienceDirect

Food Chemistry

journal homepage: www.elsevier.com/locate/foodchem

Quantification of starch content in germinating mung bean seedlings by terahertz spectroscopy

Shusaku Nakajima[a], Keiichiro Shiraga[b], Tetsuhito Suzuki[a], Naoshi Kondo[a], Yuichi Ogawa[a,*]

[a] Graduate School of Agriculture, Kyoto University, Kitashirakawa-Oiwakecho, Sakyo-ku, Kyoto 606-8502, Japan
[b] RIKEN Center for Integrative Medical Sciences (IMS), 1-7-22, Suehiro-cho, Tsurumi-ku, Yokohama, Kanagawa 230-0045, Japan

ARTICLE INFO

Keywords:
Starch
Terahertz spectroscopy
Mung bean
Hydrolysis
Quantification

ABSTRACT

To investigate the potential of terahertz spectroscopy to monitor and quantify starch in plants, terahertz spectra (3.0–13.5 THz) of mung bean plants 1–7 days after germination were examined and compared to those of starch and its constituent saccharides (standard reagents). Day 1 seedlings showed similar spectral features with standard starch, and absorption peaks gradually disappeared in the subsequent 6 day growth period. To interpret this result and identify useful peaks for starch quantification, standard starch and day 1 seedlings were hydrolyzed by α-amylase *in vitro*. Since both standard starch and seedlings showed that absorption peak at 9.0 THz disappeared after amylase hydrolysis, this peak is sensitive to changes in starch. Additionally, intensity of this peak was correlated with starch content as quantified by chemical analysis ($r = 0.98$). Our results indicate terahertz spectra of seedlings can provide an identifiable peak that is attributed to starch and not affected by the constituent saccharides.

1. Introduction

Starch is the predominant form of carbohydrate reserve in plants and mainly stored in specific organs, such as seeds, fruits, tubers and/or roots. Many of these starch storage organs play an important role in the diet of humans and starch is involved in food quality. For instance, beans have a high starch content which is converted to sugars during cooking, leading to sweetness (Rehman, Salariya, & Zafar, 2001). Similar starch conversion to sugars can be observed in banana and kiwi fruit during ripening (Cordenunsi & Lajolo, 1995; MacRae, Quick, Benker, & Stitt, 1992). Starch content is also the principal factor determining food texture after cooking (Bettelheim & Sterling, 1955). For these reasons, starch content is linked to food taste and texture.

For quantification of starch in foods researchers commonly employ a hydrolysis method (Smith & Zeeman, 2006). In this method, samples are first extracted with alcohol to remove endogenous sugars, and then dried. The extracted samples are hydrolyzed to sugars with enzymes or acid. After quantification of the converted sugars, starch content can be obtained. Although highly accurate, the method is destructive and entails complicated pretreatments, so recent studies have investigated alternative methods for starch quantification of foods.

Mung bean (*Vigna radiata* L.) seeds and sprouts are consumed mainly Asian countries, with starch being a major component in the seed. This stored seed starch begins to be degraded by enzymes after germination, and finally converted to glucose via several intermediates (Smith, Zeeman, & Smith, 2005; Swain & Dekker, 1966). Additionally, mung bean plants have the advantage of easy cultivation and rapid growth. Thus, mung bean is a good model to measure changes in starch content over time.

Spectroscopy provides not only rapid measurement without complicated pretreatments, such as extraction and purification, but also information about the molecular state and structure of the measured components. Thus, this technique is widely employed for both qualitative and quantitative measurements of metabolites in fruits and vegetables (Bamba, Fukusaki, Nakazawa, & Kobayashi, 2002; Font, Del Río-Celestino, Cartea, & De Haro-Bailón, 2005; Genkawa, Ahamed, Noguchi, Takigawa, & Ozaki, 2016). Terahertz (THz) or far-infrared (IR) regions are generally referred to as the frequency range from 100 GHz to 30 THz, which are located between the IR and microwave regions. Recent advances in light sources and detectors have enabled THz waves to be used for exploring new applications in agriculture and food science (Wang, Sun, & Pu, 2017). In contrast to conventional IR and Raman spectroscopy mainly reflecting intramolecular vibrations, spectral information in the THz region is abundant in collective modes such as intermolecular and framework vibrations, which are more directly associated with the molecular structure (Fischer, Walther, & Jepsen, 2002; Nagai, Kumazawa, & Fukasawa, 2005). For example, small molecules having a crystalline state exhibit sharp absorption

* Corresponding author.
E-mail address: ogawayu@kais.kyoto-u.ac.jp (Y. Ogawa).

https://doi.org/10.1016/j.foodchem.2019.05.065
Received 14 December 2018; Received in revised form 18 April 2019; Accepted 7 May 2019
Available online 09 May 2019
0308-8146/

peaks originated from intrinsic intermolecular forces, whereas these distinctive peaks are merged into a broad peak in amorphous state because the intrinsic forces are disentangled during changes from the crystalline to amorphous state (Hoshina et al., 2010; Walther, Fischer, & Jepsen, 2003).

Once crystalline molecules are dissolved in water, intermolecular vibration modes of the solute are disappeared for the solute-solute intermolecular forces being replaced by the solute-water interactions in solution (Nagai, Yada, Arikawa, & Tanaka, 2006; Upadhya, Shen, Davies, & Linfield, 2003). Thus, most metabolites present in plant tissues are dissolved in water and exhibit weak absorption peaks in THz regions, similar to amorphous samples (Edwards, Farwell, & Williams, 1994). On the other hand, starch is a stable molecule and has a crystalline state even in plant tissue (Hoover & Sosulski, 1985; Osundahunsi, Fagbemi, Kesselman, & Shimoni, 2003). Thus, when THz spectroscopy is used on plant samples, metabolites, such as starch, having a crystalline structure will exhibit absorption peaks, allowing it to be distinguished from the rest of the amorphous matrix. Thus, we hypothesize that THz spectroscopy can specifically detect starch absorption peaks and has the potential to be a suitable analysis method for starch quantification.

The aim of this study was to investigate whether THz spectroscopy has the potential to monitor and quantify starch in germinating seedlings. THz spectra of saccharides (standard reagents) were first measured, to identify spectral features and absorption peaks. Since saccharides consisting of monomer glucose (starch, oligosaccharides, maltose and glucose) exhibit very similar spectral features and absorption peaks in other regions (Cael, Koenig, & Blackwell, 1973; Tu, Lee, & Milanovich, 1979), we need to confirm whether THz spectroscopy can discriminate between these saccharides. Additionally, THz spectra of mung bean seedlings at different growth days were measured and compared to those of standard saccharides. After identifying absorption peaks of seedlings and spectral changes during cultivation, standard starch and mung bean seedlings were hydrolyzed by α-amylase and once again measured, to detail whether these peaks and changes can be attributed to starch degradation. Finally, a calibration model for starch quantification was developed using the peak attributed to starch.

2. Materials and methods

2.1. Chemicals

Polyethylene (PE) with a particle size 8 ± 1 μm was used to dilute samples. Potato starch was purchased from Kanto Chemical Co., Inc., and D(+)-glucose were purchased from Wako Pure Chemical Industries, Ltd. α-amylase from porcine pancreas (≥10 units/mg) and amyloglucosidase from *Aspergillus niger* (≥70 units/mg) were purchased from Sigma-Aldrich.

2.2. Sample preparation of standard saccharides

To identify spectral features, we prepared standard crystalline and amorphous saccharides for THz spectroscopy measurements. Amorphous starch was prepared according to the method (Jouppila & Roos, 1997) with some modifications. Starch suspensions containing 2% (w/w) solids were autoclaved at 121 °C to gelatinize starch granules. The resulting gels were immediately frozen and freeze-dried around −50 °C under vacuum condition (below 10 KPa) over 2 days using a freeze-drying machine (FDU-1200, Tokyo Rikakikai Co., Ltd.), and then the residual powders were used as amorphous starch. Glucose is released from starch after germination (Smith et al., 2005; Swain & Dekker, 1966) and may influence THz spectra of germinating mung bean seedlings. Thus, we also measured THz spectra of crystalline and amorphous glucose. To prepare amorphous glucose, the crystalline powders were heated at 150 °C (just above melting points) according to the method (Walther et al., 2003). After cooling, the solid was ground to a powder with a mortar and pestle.

2.3. Plant material and growth conditions

Mung bean seeds were purchased from Nakahara Seed Product Co., Ltd. and stored at room temperature in darkness until use. After removing defect seeds, the selected seeds were steeped in 70% ethanol for 5 min and then 95% ethanol for 1 min as described in our previous study (Nakajima, Shiraga, Suzuki, Kondo, & Ogawa, 2017) to sterilize any bacteria or microorganisms on the surface of the seeds. Subsequently, the sterilized seeds were rinsed for 1 min in distilled water twice, due to the negative effect of alcohol on plant growth. The seeds were germinated and cultivated on a 0.8% (w/w) agar medium (pH 5.8–6.1 adjusted with KOH) under white LED (LDL-74 × 27SW2, CCS Inc.) for 18 h light/6h dark (light intensity of 20–30 $\mu mol\, m^{-2}\, s^{-1}$ at the surface of the agar medium) at 26.0 ± 1.0 °C for 1–7 days. Since absorption of liquid water in the THz region is too strong to accurately observe inherent peaks of starch (Xu, Plaxco, & Allen, 2006), seedlings were frozen in liquid nitrogen immediately after cultivation and freeze-dried using the same freeze-dry procedure described above. Five individual seedlings were mixed, ground to powder with a mortar and pestle and kept at −80 °C until use. To obtain fundamental data, the fresh weight and lyophilized weight of seedlings 1, 4 and 7 days were also measured.

2.4. Pellet preparation and THz measurement

The obtained powder samples were mixed with PE, which is known to be a suitable diluent material for the THz region, to make sample pellets for measurement. Standard saccharides and powder plant samples were meshed, mixed with PE powder at 5% mass concentration (percentage of sample), and pressed into solid pellets with 13 mm diameter and 1.25 ± 0.05 mm thickness. Although previous study measured THz spectra of standard starch and germinating wheat seedling using a THz time-domain system between 0.1 and 3.5 THz, no distinctive absorption peaks were observed in both samples (Jiang, Ge, Lian, Zhang, & Xia, 2016). Thus, in the present study the absorbance of the pellet was measured using a Fourier transform spectrometer (FARIS-1, JASCO Corp.) equipped with a ceramic light source and a deuterated triglycine sulfate detector from 3.0 to 13.5 THz at a resolution of 0.12 THz. THz spectra were acquired under a vacuumed condition to eliminate absorption by water vapor. To enhance the SN ratio, 300 scans were recorded and averaged. This measurement was replicated three times for each pellet and the average value was used. The absorbance of pure PE pellet was also recorded as a reference. Absorption peaks were detected on the basis of second derivative spectra after the Savitzky-Golay second derivative treatment.

2.5. Preparation of hydrolyzed samples in vitro

THz spectra of standard starch and plant samples hydrolyzed by α-amylase were also measured. We found the hydrolysis method as described in 2.6 couldn't be employed in this experiment because high absorbance of sodium acetate masked the information about starch changes. Therefore, hydrolysis was performed in distilled water as follows. Standard starch and day 1 plant samples were homogenized in water, and then autoclaved at 121 °C for 30 min. After cooling, the samples were incubated at 37 °C overnight with α-amylase, and the solution had a sample-α-amylase ratio of 100:1 (w/w). We confirmed that in this ratio the influences of α-amylase on the spectrum were quite small, by measuring the absorbance of pure α-amylase. After checking for the absence of starch with indole solution, the sample was freeze-dried and the THz spectrum of the residual powder was measured in the same way as described above.

2.6. Calibration model

We compared THz spectra obtained in Section 2.4. and starch content, to develop a calibration model for starch quantification. Although second derivative treatment declines S/N ratio, it can separate overlapping peaks and correct baseline fluctuations. This data processing is often employed for designing calibration models (Genkawa et al., 2016; Rodriguez-Saona, Fry, McLaughlin, & Calvey, 2001), so we also used the Savitzky-Golay second derivative treatment and intensity in second derivative spectra for a calibration model. A linear regression model for starch content was employed, and the accuracy of the model was evaluated using the correlation coefficient (r) and root mean square error (RMSE).

Starch was converted to glucose according to the method (Smith & Zeeman, 2006), and then quantified as glucose. Samples were extracted in 80% ethanol, and incubated in a boiling bath for 5 min. After being centrifuged at 3,000 g for 5 min, the supernatant was discarded and the residual extracted three times more in the same way. The insoluble residual was dried to remove solution, homogenized in 2.0 mL water, and then autoclaved at 121 °C for 30 min. After cooling, the sample was incubated at 37 °C overnight with 2.0 mL of 200 mM sodium acetate (pH 5.5) containing α-amylase (≥1 unit) and amyloglucosidase (≥10 units).

Glucose quantification was performed using a HPLC (Shimadzu Corp.) according to the method (Ma, Sun, Chen, Zhang, & Zhu, 2014) with some modifications. The system was equipped with a LC-20AD pump, RID-20A refractive index detector, SIL-20AC autosampler, CTO-20AC column oven and C-R8A integrator. Separation was achieved on Luna NH_2 column (4.6 mm × 250 mm) and column temperature was maintained at 30 °C. The mobile phase was acetonitrile-water (70:30, v/v) at a flow rate of 1.0 mL/min. All samples were filtered through a 0.45 μm membrane filter before use, and a 10 μL of sample injected into the HPLC system. After analysis, the starch content was calculated as 90% of glucose content.

2.7. Statistical analysis

Seedling cultivation was replicated independently at least three times and 10 seedlings were used for measurement of the fresh and dry weight. Three different pellets of standard saccharides, and 5 different plant samples in each growth day were used for THz measurements.

3. Results and discussion

3.1. THz spectra of standard starch and glucose

Fig. 1 shows THz spectra of standard starch and glucose. While the THz spectra of crystalline starch showed 2 shoulder peaks at 5.0 and 7.8 THz and 4 peaks at 9.0, 10.5, 12.1 and 13.1 THz, amorphous starch had only 4 peaks at 9.0, 10.6, 12.1 and 13.1 THz. Crystalline glucose had sharp absorbance peaks due to intermolecular forces, such as hydrogen bond networks, whereas amorphous glucose exhibited a peak at 8.4 THz and two minor peaks at 12.0 and 12.7 THz due to a lack of intermolecular vibrations. Such spectral changes in glucose after amorphization have also been observed in previous THz measurements (Walther et al., 2003).

Absorption bands of saccharides between 3.0 and 13.5 THz are generally separated into two contributions; non-covalent modes such as hydrogen bond vibrations in the low frequency region and covalent skeletal deformation modes (C−C−O, C−O−C and C−C−C) in the high frequency region (Hineno, 1977; Yang, Weng, Ferraro, & Wu, 2001). Since the frequency boundary of the non-covalent and covalent modes lies around 7.5 THz (Hineno, 1977), our spectral data contains information about both vibrations. A previous THz study measured the spectra of the crystalline and the amorphous state of saccharides between 0.1 and 4.0 THz; the crystalline state has sharp peaks due to intermolecular hydrogen bonds, whereas sharp peaks disappears in amorphous due to the lack of the long-ranged structural order (Walther et al., 2003). The authors also pointed out that intramolecular vibrations should be observable in amorphous sugars in the higher frequencies, despite no such peaks below 4.0 THz.

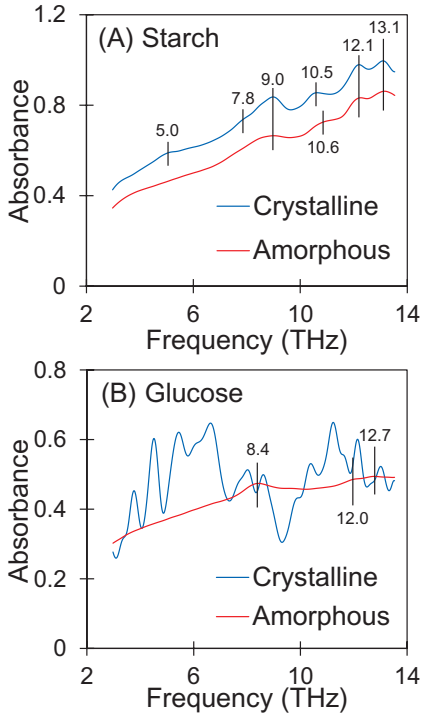

Fig. 1. Absorbance spectra of crystalline and amorphous saccharides: (A) starch; (B) glucose (n = 3). Vertical lines indicate absorption peaks of starch and amorphous glucose.

Crystalline starch has double helices stabilized by hydrogen bonds (Imberty, Buléon, Tran, & Péerez, 1991). However, heating of starch in water causes breaking of these hydrogen bonds and unwinding of the double helices, resulting in collapse of the crystalline structure (Wang, Li, Copeland, Niu, & Wang, 2015). Since no peaks at 5.0 and 7.8 THz were observed in amorphous starch (Fig. 1A), these two peaks in the low frequency region may originate from non-covalent type hydrogen bond vibrations in the double helices. On the other hand, the peak frequencies of the other 3 peaks at 9.0, 12.1 and 13.1 THz remained unchanged, indicating these vibrations are assigned to covalent modes, which are little affected by crystalline/amorphous structures. The peak at 10.5 THz observed in crystalline starch shifted slightly to a higher frequency at 10.6 THz in the amorphous state. While structural changes in long-ranged order (intermolecular vibrations) are observed as appearance and disappearance and/or intensity changes in the peaks, changes in short-ranged order (intramolecular vibrations) are observed as peak shifts in the THz region (Nagai et al., 2005). The shift observed in starch after amorphization may originate from differences in starch structures and intramolecular covalent modes, but it should be noted that we did not perform the analysis of starch structure in this study. Thus, it is difficult to attribute the cause of this peak shift after amorphization from our data.

3.2. Growth of mung bean seedlings

The growth of the seedlings during the first 7 days of cultivation is shown in Fig. 2. The radicle started to elongate after germination and the formation of green leaves, stem and lateral roots was observed in 4 day seedlings. The length of seedlings and number of lateral roots continued to increase during cultivation. In addition, some cotyledons

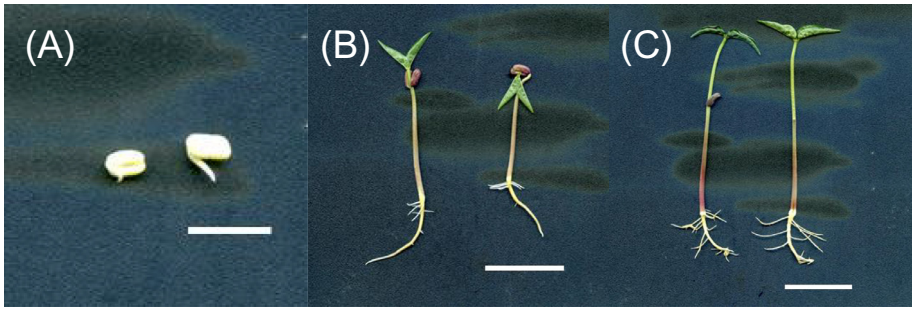

Fig. 2. Growth of mung bean seedlings: (A) day 1, bar = 2 cm; (B) day 4, bar = 4 cm; (C) day 7, bar = 4 cm.

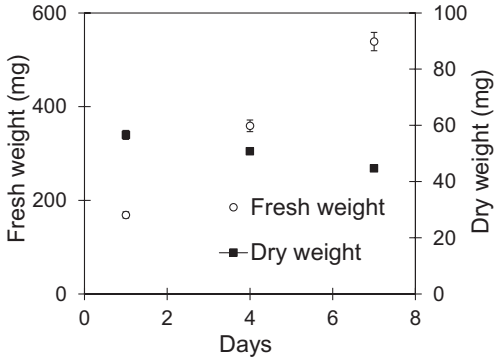

Fig. 3. Fresh and dry weight of seedlings (n = 10). Data are expressed as means ± standard error, and error bar indicates individual differences of 10 seedlings.

abscised from the stem after 7 days of cultivation. The fresh weight of seedlings continued to increase, while dry weight of lyophilized seedlings slightly decreased during the 7 days of cultivation (Fig. 3). The starch contents of the seedlings (average of 5 samples) continued to decrease during the cultivation (55.6, 50.6, 41.4, 34.4, 16.6, 7.8 and 3.0% at day 1, 2, 3, 4, 5, 6 and 7, respectively).

3.3. THz spectra of mung bean seedlings

The THz spectra of mung bean seedlings on different cultivation days are shown in Fig. 4. Although we measured seedlings at day 1–7, only THz spectra of seedlings at day 1, 4 and 7 are shown where spectral changes were clearly observable. The frequencies of 2 shoulder and 4 peaks observed in mung bean seedlings at day 1 were consistent with those of standard starch (Fig. 1), although the two peaks at 7.8 and

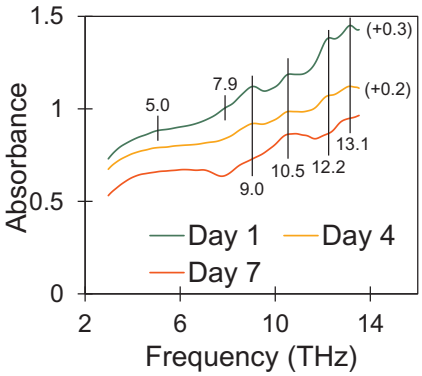

Fig. 4. Absorbance spectra of mung bean seedlings at different growth days (n = 5). The spectra of day 1 and 4 are offset vertical for peak clearly, +0.3 and +0.2 respectively. Vertical lines indicate absorption peaks observed in seedlings.

12.1 THz in standard starch were shifted slightly to a higher frequency at 7.9 and 12.2 THz in seedlings, respectively. Additionally, the peak width and intensity gradually broadened and weakened during the 7 days of cultivation. Since the expression of many metabolites have been reported after germination (Jom, Frank, & Engel, 2011), one possible explanation for these spectral changes in the mung bean seedlings is just due to the dilution of the starch in the seedlings with the increase of other metabolites, and not due to starch degradation. However, the dry weight of seedlings did not increase during cultivation (Fig. 3), so reduced peak intensities during the cultivation were not due to other metabolites. An alternative hypothesis is that the 6 peaks observed in day 1 seedlings are inherent in starch and reflect starch degradation over the cultivation period. If this hypothesis is true, these peaks can be useful indicators for starch quantification. From this point of view, the 4 peaks in the higher frequencies (9.0, 10.5, 12.2 and 13.1 THz) are supposed to be more effective to estimate starch content, rather than weak shoulders at 5.0 and 7.9 THz. To further confirm the validity of these 4 peaks as useful indicators for starch quantification, the THz spectra of hydrolyzed starch and day 1 seedlings were also measured as described in Section 3.4.

In germinating mung bean seedlings, stored seed starch is converted to glucose via several intermediates (Smith et al., 2005; Swain & Dekker, 1966). An increase in glucose content has been found in the cotyledon and the embryonic axis of germinating mung beans (Kuo, VanMiddlesworth, & Wolf, 1988). Despite not being experimentally confirmed in this study, it is no wonder to consider that day 4 and 7 seedlings had higher levels of the glucose content than day 1 seedlings. Since glucose may form complexes with other metabolites in plant tissues, any glucose peaks inherent in crystalline and amorphous are not observed in day 4 and 7 (Fig. 4).

In plant tissues, glucose plays several roles in not only nutrition, but also enhancing the stability and solubility of other metabolites by conjugating with them; a process termed glycosylation. Examples of this glycosylation are observed when glucose conjugates with steroids, phenolics, flavonoids and phytohormones in plant tissues (Gachon, Langlois-Meurinne, & Saindrenan, 2005; Wang, 2009). Furthermore, THz spectra of standard sugars and metal-sugar complexes between 1.5 and 19.5 THz indicate that absorption peaks of metal-sugar complexes became broader or absent, compared to standard sugars (Yang et al., 2008). Though no reports on the THz spectra of conjugated glucose in plants tissues could be found, it is thought that they also have no distinct absorption peaks. Therefore, the absence of glucose-derived peaks in day 4 and 7 seedlings is a consequence of the conjugation.

3.4. THz spectra of hydrolyzed samples

THz spectra of hydrolyzed starch and seedlings are showed in Fig. 5. For reasons mentioned above, we focus on the changes in the 4 peaks in the high frequency region. The absorption peak at 9.0 and 10.5 THz were hardly visible, but alternative peaks at 8.4 and 11.0 THz were recognized in the hydrolyzed starch. On the other hand, the two peaks at 12.1 and 13.1 THz were still observable after hydrolysis, although

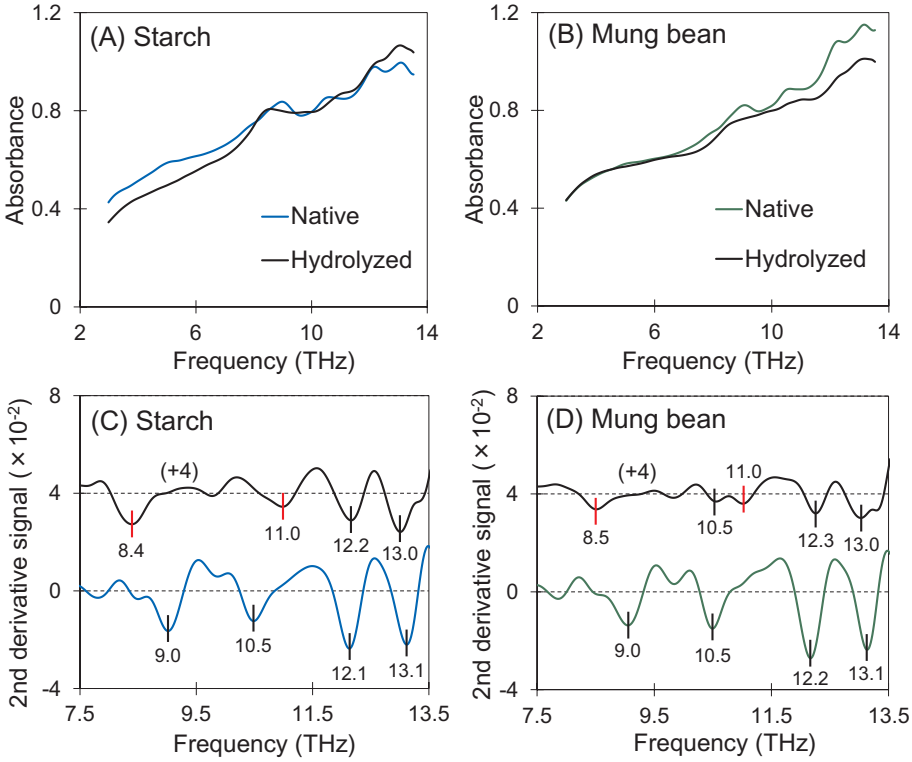

Fig. 5. Absorbance spectra of hydrolyzed and native samples: (A) Starch (n = 3); (B) mung bean seedlings (n = 5). Second derivative spectra in the range of 7.5–13.5 THz: (C) Starch; (D) mung bean seedlings. The spectra of hydrolyzed samples are offset vertically (+4). Vertical lines indicate absorption peaks, and new peaks after hydrolysis were remarked by red lines.

peak positions and intensities were slightly shifted and weakened, respectively, compared to native starch (before hydrolysis). Since starch is hydrolyzed into oligosaccharides and maltose by amylase, we also measured standard oligosaccharides and maltose with amorphous state and confirmed absorption peaks around 8.5, 11.0, 12.0 and 13.0 THz (see Fig. S1). Previous studies have shown that in 7.5–13.5 THz range, polysaccharides exhibit skeletal deformation modes, commonly called ring vibrations (Hineno, 1977; Tu et al., 1979; Yang et al., 2001). Thus, these new peaks observed in hydrolyzed starch could be attributed to covalent skeletal vibrations of oligosaccharides and maltose that result from conversion of starch.

As seen from Fig. 5, hydrolyzed mung bean seedlings showed different spectral changes, compared to those of standard starch. While the peak at 9.0 THz was unobservable in the hydrolyzed samples, the other three peaks at 10.5, 12.2 and 13.1 THz remained after hydrolysis. An obvious difference from the standard starch is that the peak at 10.5 THz is remained (albeit very weak) in the THz absorbance spectra of hydrolyzed mung bean seedlings. This is possibly attributed to other metabolites in seedlings, which incidentally give rise to an absorption peak around 10.5 THz. The most important finding here is that the peak at 9.0 THz inherent in starch is completely vanished after hydrolysis, suggesting that it is the only useful indicator to monitor and quantify starch in germinating seedlings, while the other three peaks are not.

Although the starch content of day 1 seedlings is 55.6%, the intensities of the 4 peaks in native mung bean seedling are similar to or higher than those of native starch (Fig. 5(C), (D)). This result indicates that the molar absorptivity (i.e. absorption coefficient normalized by molar concentration) of native mung bean seedlings is much higher than that of native starch. The reason for this may be that the structure of native *potato* starch is different from that of *mung bean* one, and THz absorbance reflects the starch structure. More specifically, starch is classified into three types (A-, B- and C-type), depending on the crystal structures of the starch granules. X-ray diffraction analysis has shown there are structural differences between potato (B-type) and mung bean starch (C-type) (Hoover, Li, Hynes, & Senanayake, 1997; Sarko & Wu, 1978). Additionally, we confirmed that these structural differences influence spectral features and peak intensities in the THz region, and higher peak intensities were obtained in A-type starch versus B-type starches (see Fig. S2). We could not obtain and measure standard C-type starch in this study because it is commercially unavailable. Nevertheless, it is known that the crystalline structure of C-type starch is a combination of A- and B-types. Thus, it is reasonably expected that mung bean starch may have higher peak intensities, compared to potato starch, which results in the higher molar absorptivity of starch in mung bean seedlings.

3.5. Quantification of starch

Fig. 6 shows a comparison between estimated and measured starch content for the same samples. The estimated starch contents were obtained from peak intensity at 9.0 THz in the second derivative spectra. Starch content using the reference method ranged from 1.8 to 57.0%,

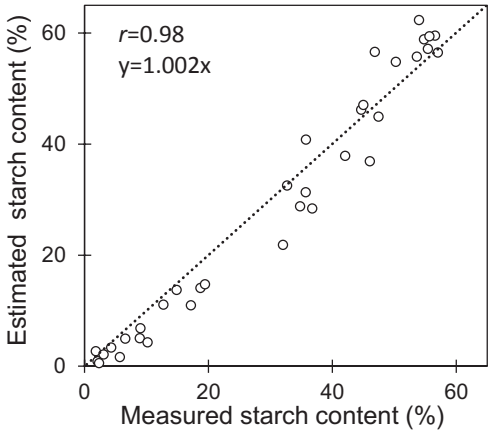

Fig. 6. Correlation between estimated starch content using peak intensity at 9.0 THz in second derivative spectra and measured starch content obtained by chemical analysis (n = 35).

where the model had r of 0.98 and RMSE of 4.7%. Although previous research developed calibration models for starch quantification in maize grain using a spectroscopic technique in other regions (Orman & Schumann, 1991), the accuracy was lower than in the present study (r^2 = 0.58–0.78). Therefore, the results indicate THz spectroscopy has the potential to be selective and accurate tool for starch quantification in foods, as hypothesized.

4. Conclusions

In this study we found mung bean seedlings give rise to an identifiable peak at 9.0 THz that is assigned to a covalent vibration of starch and is not affected by the constituent saccharides. According to this peak, starch quantification was successfully achieved (r = 0.98). Although in this preliminary study THz measurements used a destructively sampling procedure, the data demonstrates the new potential of THz technology to monitor and quantify starch in the plant matrix without the need for purification pretreatments. Based on these results, further investigations will need to be undertaken to confirm the viability of nondestructive measurements.

Declaration of Competing Interest

The authors have declared no conflicts of interest.

Acknowledgements

The authors thank Prof. Garry John Piller (Kyoto University) for reading this report and helpful suggestions. This work was supported by JSPS KAKENHI Grant Number 16H05010 and 17J08363.

Appendix A. Supplementary data

Supplementary data to this article can be found online at https://doi.org/10.1016/j.foodchem.2019.05.065.

References

Bamba, T., Fukusaki, E., Nakazawa, Y., & Kobayashi, A. (2002). In-situ chemical analyses of trans-polyisoprene by histochemical staining and Fourier transform infrared microspectroscopy in a rubber-producing plant, *Eucommia ulmoides* Oliver. *Planta, 215*(6), 934–939.

Bettelheim, F. A., & Sterling, C. (1955). Factors associated with potato texture. I. Specific gravity and starch content. *Journal of Food Science, 20*(1), 71–79.

Cael, S. J., Koenig, J. L., & Blackwell, J. (1973). Infrared and raman spectroscopy of carbohydrates : Part III: Raman spectra of the polymorphic forms of amylose. *Carbohydrate Research, 29*(1), 123–134.

Cordenunsi, B. R., & Lajolo, F. M. (1995). Starch breakdown during banana ripening: Sucrose synthase and sucrose phosphate synthase. *Journal of Agricultural and Food Chemistry, 43*(2), 347–351.

Edwards, H. G. M., Farwell, D. W., & Williams, A. C. (1994). FT-Raman spectrum of cotton: A polymeric biomolecular analysis. *Spectrochimica Acta Part A: Molecular Spectroscopy, 50*(4), 807–811.

Fischer, B. M., Walther, M., & Jepsen, P. U. (2002). Far-infrared vibrational modes of DNA components studied by terahertz time-domain spectroscopy. *Physics in Medicine and Biology, 47*(21), 3807–3814.

Font, R., Del Río-Celestino, M., Cartea, E., & De Haro-Bailón, A. (2005). Quantification of glucosinolates in leaves of leaf rape (*Brassica napus* ssp. *pabularia*) by near-infrared spectroscopy. *Phytochemistry, 66*(2), 175–185.

Gachon, C. M. M., Langlois-Meurinne, M., & Saindrenan, P. (2005). Plant secondary metabolism glycosyltransferases: The emerging functional analysis. *Trends in Plant Science, 10*(11), 542–549.

Genkawa, T., Ahamed, T., Noguchi, R., Takigawa, T., & Ozaki, Y. (2016). Simple and rapid determination of free fatty acids in brown rice by FTIR spectroscopy in conjunction with a second-derivative treatment. *Food Chemistry, 191*(15), 7–11.

Hineno, M. (1977). Infrared spectra and normal vibration of β-D-glucopyranose. *Carbohydrate Research, 56*(2), 219–227.

Hoover, R., Li, Y. X., Hynes, G., & Senanayake, N. (1997). Physicochemical characterization of mung bean starch. *Food Hydrocolloids, 11*(4), 401–408.

Hoover, R., & Sosulski, F. (1985). Studies on the functional characteristics and digestibility of starches from *Phaseolus vulgaris* biotypes. *Starch - Stärke, 37*(6), 181–191.

Hoshina, H., Morisawa, Y., Sato, H., Kamiya, A., Noda, I., Ozaki, Y., & Otani, C. (2010). Higher order conformation of poly(3-hydroxyalkanoates) studied by terahertz time-domain spectroscopy. *Applied Physics Letters, 96*(10), 3–6.

Imberty, A., Buléon, A., Tran, V., & Péerez, S. (1991). Recent advances in knowledge of starch structure. *Starch - Stärke, 43*(10), 375–384.

Jom, K. N., Frank, T., & Engel, K. H. (2011). A metabolite profiling approach to follow the sprouting process of mung bean (*Vigna radiata*). *Metabolomics, 7*(1), 102–117.

Jouppila, K., & Roos, Y. H. (1997). The physical state of amorphous corn starch and its impact on crystallization. *Carbohydrate Polymers, 32*(2), 95–104.

Jiang, Y., Ge, H., Lian, F., Zhang, Y., & Xia, S. (2016). Early detection of germinated wheat grains using terahertz image and chemometrics. *Scientific Reports, 6*, 21299.

Kuo, T. M., VanMiddlesworth, J. F., & Wolf, W. J. (1988). Content of raffinose oligosaccharides and sucrose in various plant seeds. *Journal of Agricultural and Food Chemistry, 36*(1), 32–36.

Ma, C., Sun, Z., Chen, C., Zhang, L., & Zhu, S. (2014). Simultaneous separation and determination of fructose, sorbitol, glucose and sucrose in fruits by HPLC-ELSD. *Food Chemistry, 145*, 784–788.

MacRae, E., Quick, W. P., Benker, C., & Stitt, M. (1992). Carbohydrate metabolism during postharvest ripening in kiwifruit. *Planta, 188*(3), 314–323.

Nagai, N., Kumazawa, R., & Fukasawa, R. (2005). Direct evidence of inter-molecular vibrations by THz spectroscopy. *Chemical Physics Letters, 413*(4–6), 495–500.

Nagai, M., Yada, H., Arikawa, T., & Tanaka, K. (2006). Terahertz time-domain attenuated total reflection spectroscopy in water and biological solution. *International Journal of Infrared and Millimeter Waves, 27*(4), 505–515.

Nakajima, S., Shiraga, K., Suzuki, T., Naoshi, K., & Ogawa, Y. (2017). Chlorophyll, carotenoid and anthocyanin accumulation in mung bean seedlings under clinorotation. *Microgravity Science and Technology, 29*(6), 427–432.

Orman, B. A., & Schumann, R. A. (1991). Comparison of near-infrared spectroscopy calibration methods for the prediction of protein, oil, and starch in maize grain. *Journal of Agricultural and Food Chemistry, 39*(5), 883–886.

Osundahunsi, O. F., Fagbemi, T. N., Kesselman, E., & Shimoni, E. (2003). Comparison of the physicochemical properties and pasting characteristics of flour and starch from red and white sweet potato cultivars. *Journal of Agricultural and Food Chemistry, 51*(8), 2232–2236.

Rehman, Z., Salariya, A. M., & Zafar, S. I. (2001). Effect of processing on available carbohydrate content and starch digestibility of kidney beans (*Phaseolus vulgaris* L.). *Food Chemistry, 73*(3), 351–355.

Rodriguez-Saona, L. E., Fry, F. S., McLaughlin, M. A., & Calvey, E. M. (2001). Rapid analysis of sugars in fruit juices by FT-NIR spectroscopy. *Carbohydrate Research, 336*(1), 63–74.

Sarko, A., & Wu, H. C. H. (1978). The crystal strucutre of A-, B- and C-polymorphs of amylose and starch. *Starch - Stärke, 30*(3), 73–78.

Smith, A. M., & Zeeman, S. C. (2006). Quantification of starch in plant tissues. *Nature Protocols, 1*(3), 1342–1345.

Smith, A. M., Zeeman, S. C., & Smith, S. M. (2005). Starch degradation. *Annual Review of Plant Biology, 56*(1), 73–98.

Swain, R. R., & Dekker, E. E. (1966). Seed germination studies II. Pathways for starch degradation in germinating pea seedlings. *Biochimica et Biophysica Acta (BBA), 122*(1), 87–100.

Tu, A. T., Lee, J., & Milanovich, F. P. (1979). Laser-Raman spectroscopic study of cyclohexaamylose and related compounds: Spectral analysis and structural implications. *Carbohydrate Research, 76*(1), 239–244.

Upadhya, P. C., Shen, Y. C., Davies, A. G., & Linfield, E. H. (2003). Terahertz time-domain spectrsocpy o glucose and uric acid. *Journal of Biological Physics, 29*(2–3), 117–121.

Walther, M., Fischer, B. M., & Jepsen, P. U. (2003). Noncovalent intermolecular forces in polycrystalline and amorphous saccharides in the far infrared. *Chemical Physics, 288*(2–3), 261–268.

Wang, K., Sun, D. W., & Pu, H. (2017). Emerging non-destructive terahertz spectroscopic imaging technique: Principle and applications in the agri-food industry. *Trends in Food Science and Technology, 67*, 93–105.

Wang, S., Li, C., Copeland, L., Niu, Q., & Wang, S. (2015). Starch Retrogradation: A Comprehensive Review. *Comprehensive Reviews in Food Science and Food Safety, 14*(5), 568–585.

Wang, X. (2009). Structure, mechanism and engineering of plant natural product glycosyltransferases. *FEBS Letters, 583*(20), 3303–3309.

Xu, J., Plaxco, K. W., & Allen, S. J. (2006). Absorption spectra of liquid water and aqueous buffers between 0.3 and 3.72THz. *The Journal of Chemical Physics, 124*(3), 036101.

Yang, L., Weng, S., Ferraro, J. R., & Wu, J. (2001). Far infrared study of some mono- and disaccharides. *Vibrational Spectroscopy, 25*(1), 57–62.

Yang, L., Sun, H., Weng, S., Zhao, K., Zhang, L., Zhao, G., ... Jia'er, C. (2008). Terahertz absorption spectra of some saccharides and their metal complexes. *Spectrochimica Acta - Part A: Molecular and Biomolecular Spectroscopy, 69*(1), 160–166.